## *Hetero- and low-dimensional structures*

# Electron levels of defects in In(Ga)As/(In)GaAs nanostructures: A review

**O.I. Datsenko[1], V.M. Kravchenko[1], S. Golovynskyi[2,*]**

[1]*Taras Shevchenko National University of Kyiv, Physics Faculty, 01601 Kyiv, Ukraine*
[2]*College of Physics and Optoelectronic Engineering, Shenzhen University, 518060, Shenzhen, P.R. China*
[*]*Corresponding author e-mail: serge@szu.edu.cn*

**Abstract.** The data on electron levels induced by defects in In(Ga)As/(In)GaAs nanostructures, their localization, activation energy and identification have been systematically reviewed. Point defects inherent to GaAs and found in the (In)GaAs-based nanostructures have been listed, and their classification has been clarified, including EB3, EL2, EL3, EL4 (M4), EL5, EL6 (M3), EL7, EL8, EL9 (M2), EL10 (M1), EL11 (M0) and M00. The effect of the interfaces on the formation of different types of extended defects has been described. All the levels of electron traps found in heterostructures with quantum wells, wires and dots by deep level spectroscopies have been collected in a table with indication of the detection technique, object, location in the structure and their origin assumed. This overview can be useful as a reference material for researchers who study these nanostructures.

**Keywords:** InAs/GaAs, nanoheterostructures, defect, electron state, deep level spectroscopy.

## 1. Introduction

$A^{III}B^{V}$ semiconductor nanostructures are widely used as an active element in electronic device design. In particular, In(Ga)As nanoobjects embedded in GaAs or InGaAs find their application in optoelectronics as materials for effective photodetectors [1, 2], light sources [3, 4] and solar cells [5, 6]. Naturally, a large amount of scientific works is devoted to defects in such structures, as defects mainly decrease the efficiency of optoelectronic devices to a significant extent. On the other hand, the defects are also found to improve the photoresponse of intermediate-band solar cells, being a competitive way for effective recombination in quantum dots (QDs) [7, 8].

Electron levels of defects in semiconductor nanostructures are studied using a variety of methods. Investigation of absorption, photoelectric or lumi-nescence spectra [9–13] provides information about the distance from defect levels to the energy bands involved in electron transitions. The advanced methods using temperature dependences of different parameters that are, in turn, dependent on the activation energy ($E_a$) of electron levels allow one to obtain additional parameters of defect centers, *e.g.*, the capture cross-section. Most of researchers employ the deep level transient spectroscopy (DLTS) technique (Fig. 1) [14–16]. Optical methods of defect level filling are also applied in deep level thermally stimulated conductivity (TSC) spectroscopy (Fig. 2) [17–19] and photo-induced current transient spectroscopy (PICTS) [18, 20] (Fig. 3). Admittance [21] and noise spectroscopy (DLNS) [22] techniques find their use in deep level detection. Varying the measurement conditions, these methods allow to determine the spatial localization of defect centers. The depth profiles of defect concentration can also be indirectly estimated by means of $C–V$ measurements [21, 22].

Despite extensive investigation of defects in In(Ga)As/GaAs nanostructures, their identification is associated with certain difficulties caused, for example, by localization of defects near structure features like a surface or strained heterointerface [24]. As a result, the response of a defect level, especially a shallow one, could be lost against the background of the signal of nanostructure quantum levels [25]. Furthermore, some known defects have $E_a$ with close values, resulting in overlapping of their bands, so that the thermally-driven methods provide insufficient resolution to distinguish these defects. Consequently, different origins could be attributed to the same defects by different authors. For example, similar DLTS peaks have been related to
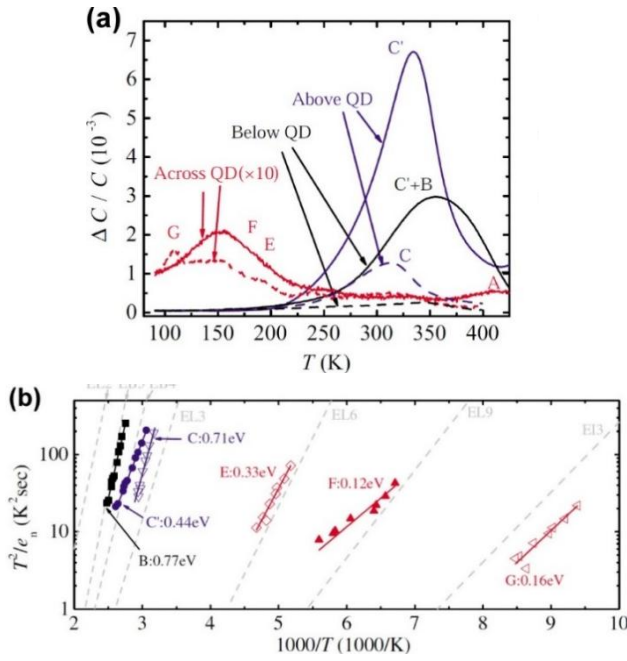
**Fig. 1.** DLTS spectra of different regions in $In_{0.15}Ga_{0.85}As/$ GaAs QD structures (a) and Arrhenius plots of the deep traps observed in the structures (b). The deep levels reported in the literature with similar signatures are also plotted as dotted lines for comparison. Reprinted from Asano *et al.* [16], with the permission of © 2010 AIP Publishing.
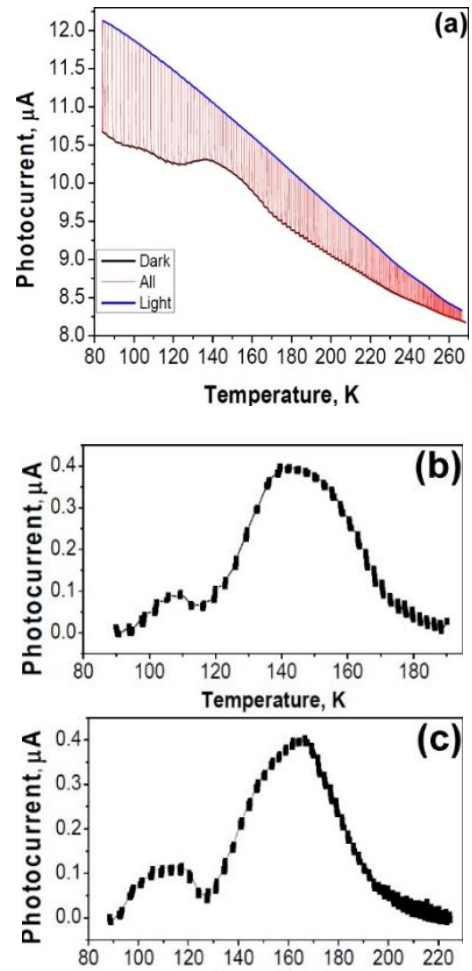


**Fig. 2.** TSC spectra of an InAs/$In_{0.15}Ga_{0.85}As$ QD structure measured after the resonant QD excitation at 1.01 eV (a) and the simultaneous $In_{0.15}Ga_{0.85}As$ buffer and QD array excitation at 1.3 eV with different times of illumination/delay (b). Estimated activation energies of the traps in eV and their interpretations are given near the vertical arrows and bands. Reproduced from Golovynskyi *et al.* [23], with the permission of © 2019 IOP Publishing, all rights reserved.



**Fig. 3.** Temperature-driven photocurrent of an $In_{0.38}Ga_{0.62}As$/GaAs quantum wire structure under modulated excitation at 1.35 eV (a) and extracted PICTS spectra under excitation at 1.35 eV (b) and 1.65 eV (c). Reprinted from Iliash *et al.* [18], open access © 2016, V. Lashkaryov Institute of Semiconductor Physics, National Academy of Sciences of Ukraine.
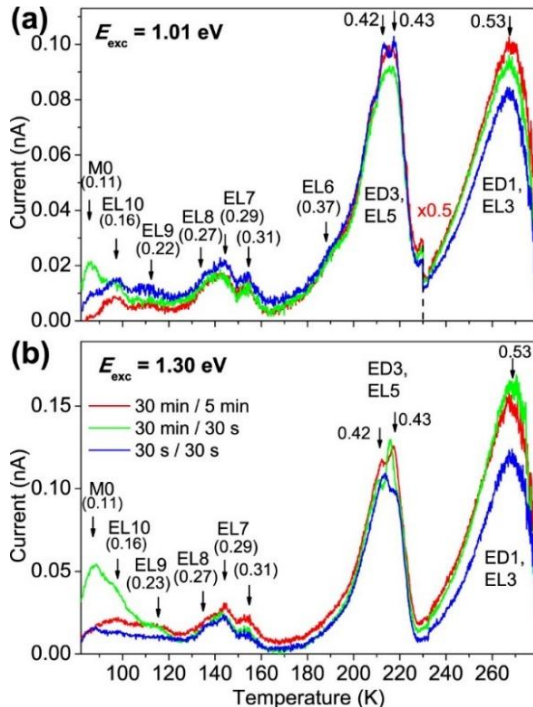
Lang's defects M2 [26], M3 [27] and M4 [28]. Thus, it is reasonable to combine several methods of investigation to make defect localization and elucidation of their nature better [28].

The aim of this review is to put in order the data on electron levels induced by defects in In(Ga)As/(In)GaAs nanostructures, their localization, $E_a$ and identification. The most of information on defects are provided in the form of a table.

## 2. GaAs-inherent point defects in (In)GaAs-based nanostructures

Point defects (PDs) in InGaAs semiconductors are the well-known intrinsic PDs of GaAs. They are widely studied since 1974, when Lang [29] suggested DLTS to study deep levels in semiconductors. The researchers who study InGaAs defects equally use the following two kinds of their cataloging.

*Datsenko O.I., Kravchenko V.M., Golovynskyi S. Electron levels of defects in In(Ga)As/(In)GaAs nanostructures…*

**Table.** Attribution of the electron levels to GaAs point defects or related extended defects.

| Level depth below $E_c$ (eV) | Nomination by Martin (Lang) | Possible origin |
|---|---|---|
| $\gtrsim 0.90$ | EB3 | $As_{Ga}$ antisite defect, DFT [36] |
| 0.9…0.65 | EL2 family (M7, M8) | Ga vacancy, $V_{Ga}$, DFT [36] |
| 0.60…0.50 | EL3 (M5, M6) | |
| 0.46…0.50 | EL4 (M4) | $Ga_{As}$ antisite [36] |
| 0.40…0.43 | EL5 | |
| 0.33…0.40 | EL6 (M3) | |
| 0.28…0.30 | EL7 (M2) | |
| 0.27…0.28 | EL8 | Frenkel pair $V_{As}$-$As_i$, [34] |
| 0.22…0.24 | EL9 | Frenkel pair $V_{As}$-$As_i$ |
| 0.15…0.20 | EL10 (M1) | Frenkel pair $V_{As}$-$As_i$ |
| 0.08…0.12 | (M0) | $V_{As}$ [51] |
| 0.030…0.045 | (M00) | $V_{As}$ [50, 51] |

The first one is Lang's classification [30] in which nine defects are marked M0-M8 with $E_a$ below the GaAs conduction band edge ($E_c$) from $E_c – 0.1$ to 0.85 eV. At the same time, a significant part of scientists prefers the table of Martin *et al.* [31], who, apart from their own results, analyzed data of other works as well. The latter classification, marked EL (electron level), is more complete, though slightly confused, and does not include (in the beginning) the shallowest (M0) defect by Lang. Origins of all these defects are reported as the native defects and their complexes.

As seen in Table, the researchers found different GaAs defects in In(Ga)As/(In)GaAs nanostructures. The deepest one is EL2 by Martin [31] and corresponds to M8 defect in Lang's classification [30]. It is the most studied recombination center in GaAs [32]. Its energy location by transient spectroscopy techniques was reported in GaAs to be from about $E_c – 0.70$ [33] to 0.93 eV [34], though photocapacitance spectroscopy detected its value to exceed 1 eV for some GaAs samples [35]. These energy responses are attributed to the electron transfer from $EL2^0$ to the conduction band, resulting in the $EL2^+$ state, the level of which is close to $E_v + 0.67$ eV at 77 K [35]. The next ionized state $EL2^{++}$ is located at $E_v + 0.47$ eV. The intra-center transitions in the neutral state occur above 1 eV [32].

It should be mentioned, however, that Martin *et al.* [31] observed a state at $E_c – 0.825$ eV and named it EL2 defect, while the name EB3 was given to another one at 0.9 eV. In addition, recent DFT calculations by Bacuyag *et al.* [36] show for Ga vacancy ($V_{Ga}$) to have a level at $E_c – 0.82$ eV and for $As_{Ga}$ antisite defect to have a level at 0.97 eV. Bacuyag *et al.* attributed these states to EL2 and EB3, respectively. Therefore, we relate the deepest states of GaAs at $\gtrsim 0.9$ eV to EB3.

EL3 electron trap (M5 or M6 by Lang) is referred to $E_c – 0.55$ to 0.65 eV [34]. It is mainly associated with As vacancy or a complex related to this defect [34, 37]. EL4 (M4) has $E_a$ from 0.48 to 0.52 eV [30, 38] and is attributed to ionized arsenic antisite $As_{Ga}^{++}$ defect [39] or defect complexes involving $V_{As}$ [40]. Also, Bacuyag *et al.* [36] calculated that $Ga_{As}$ antisite introduces a level at $E_c – 0.52$ eV and attributed it to EL4.

EL5 trap is mentioned at $E_a$ ranging from 0.37 to 0.45 eV [34, 41] and attributed to PD complexes originating from vacancies of As and/or Ga [34, 42]. Similar defects are reported [24, 43] as origins for EL6 ($E_a$ from 0.32 [44] to 0.38 eV [34]) and EL7 ($E_a$ from 0.27 [34] to 0.31 eV [45]). M3 ($E_c – 0.30$ eV) [30] is usually associated with both of these Martin's defects. EL7 trap can be also associated with other Lang's defect M2, $E_a$ of which ~0.29 eV was first obtained quite approximately from the respective peak temperature rather than Arrhenius plot [30]. EL5, EL6 and EL7 are often referred to the so-called EL6 group, because they occur in close proximity to each other and are nearly always present together in the as-grown material [34, 46].

EL8 trap was also sometimes reported in the InAs/GaAs nanostructures [47] and also equated with M3, though its $E_a$ of 0.275 eV [31] notably differs from that of M3 of 0.30 eV [30], and it would be more adequate to associate it with a shallower M2 (0.29 eV). Frenkel pairs $V_{As}$-$As_i$ are assigned as responsible for EL8 peaks in the deep level spectra [34]. Some of researchers report less $E_a$ within 0.22…0.25 eV interval for this trap [34], maybe confusing this defect with a shallower EL9 one, which is hardly observable by DLTS.

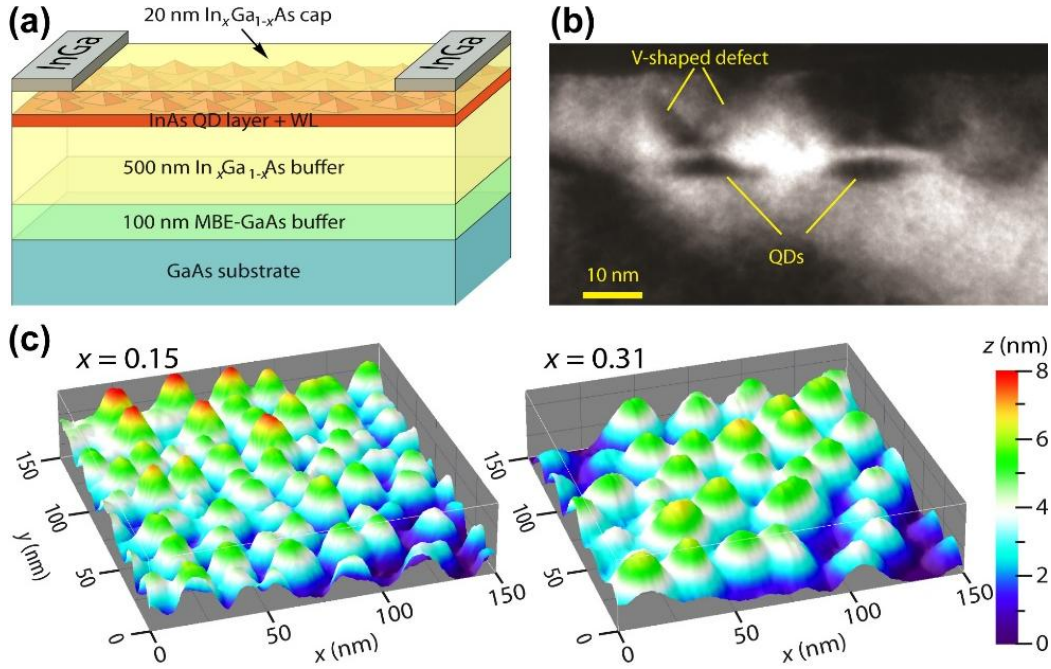EL9 is found at $E_c – (0.22…0.24$ eV) [48] and associated with PD complexes involving As vacancy [45].

**Fig. 4.** (a) Scheme of the InAs/In$_x$Ga$_{1-x}$As QD structures. (b) HRTEM images of near-surface (110) cross-section of the InAs/In$_{0.15}$Ga$_{0.85}$As sample. (c) AFM images for similar uncapped structures. Reproduced from Golovynskyi *et al.* [23], with the permission of © 2019 IOP Publishing, all rights reserved.

The traps with $E_a$ within 0.22…0.24 eV are usually observed after optical excitation (TSC or PICTS) rather than DLTS in both bulk GaAs [49] and nanostructures (see Table S1 in Supplementary Materials).

Numerous shallow levels at $E_c - (0.11…0.18$ eV$)$ [34, 41] are attributed mainly to M1 trap (0.19 eV) by Lang [30], perhaps because there are several electron traps in Martin's classification [31] which have similar $E_a$. These are EL10 and EL11 (0.17 eV) as well as EL15 (0.15 eV). These shallow traps are attributed to isolated As vacancies or distant Frenkel pairs V$_{As}$-As$_i$ [50].

The depth of M0, the shallowest of the traps classified by Lang, is reported to be about 0.08 eV [31]. A similar trap at $0.10 \pm 0.02$ eV is related to V$_{As}$ [51]. Finally, DeJule *et al.* found a shallower trap about $E_c - 0.03$ eV of GaAs [52] and, respectively, named it M00. Most researchers relate these shallow traps at $E_c - (0.030…0.045$ eV$)$ to V$_{As}$ [50, 51]. The studies reaching liquid helium temperatures in deep level spectroscopy occasionally detect similar traps in the discussed nanostructures as well [53].

## 3. Release of strains in nanostructures and extended defects

Any heterojunction implies a misfit of lattice constants at the interface, which causes the mechanical stresses being the higher, the larger the misfit. The largest stresses in a heterostructure are near the interface itself, decreasing with the distance from the junction on both sides. When growing an In(Ga)As material on (001) GaAs that has a lower lattice parameter, misfit dislocations (MDs) in two orthogonal $\langle 110 \rangle$ directions [54] are formed near

the interface on the GaAs side, whereas threading dislocations (TDs) propagate from the interface to the surface through the upper layer [24].

When the amount of an In(Ga)As covering material is low but higher than the threshold value, the misfit leads to formation of local nano-islands (Fig. 4). The self-assembled QDs tend to be elongated along one of the $\langle 110 \rangle$ directions [55], which allows one to grow a net of QD chains or quantum wires (QWRs) under certain growth conditions [56]. When capping the In(Ga)As nanoobjects by a GaAs layer, a set of TDs propagates through the cap layer from QDs. Pairs of TDs (V-shape defects, Figs 4b, 5a) are found to nucleate at large size islands, the so-called ripened QDs [57, 58]. It is shown by AFM plane images and TEM cross-section ones that their branches travel in opposite directions on the $(1-1-1)$ and $(111)$ glide planes, part of dislocations with orthogonal orientation along $[1-10]$, gliding on the $(1-11)$ and $(-1-11)$ planes, appear at high InAs coverages. Interaction of different V-shape defects can lead to their self-annihilation, however, a significant part of them can reach the surface of structure even at the cap thickness above 500 nm [56]. Beside the V-shape defects, squared-shaped stacking faults are observed on AFM plane images (Fig. 6) [59].

Extended defects (EDs) can be an origin of energy levels in the semiconductor bandgap. For example, Wosiński [61] found a state at $E_c - 0.68$ eV in GaAs crystal and named it ED1. Its DLTS peak amplitude reveals a logarithmic dependence on filling pulse duration ($t_p$), which is an attribute of EDs, where the traps are configured as interacting linear arrays.
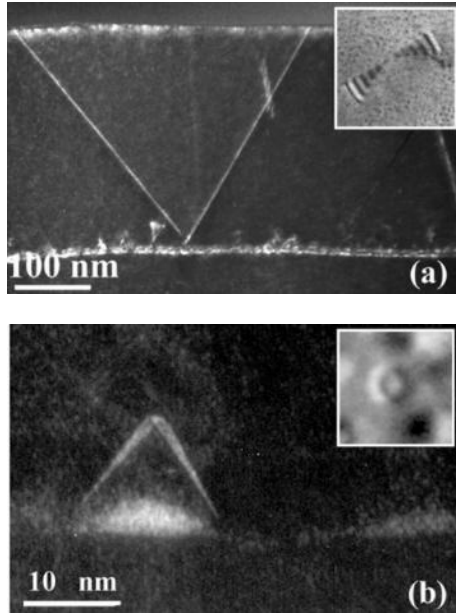
**Fig. 5.** Cross-section TEM images of the structural defects nucleating at the QD/InGaAs interface: (a) V-shaped defects; (b) closed-shaped defects surrounding single dots. The insets: 500×500 nm and 50×50 nm sized, respectively, showing the plan views of the defects. Reprinted from *Seravalli et al.* [60], with the permission of © 2010 AIP Publishing.
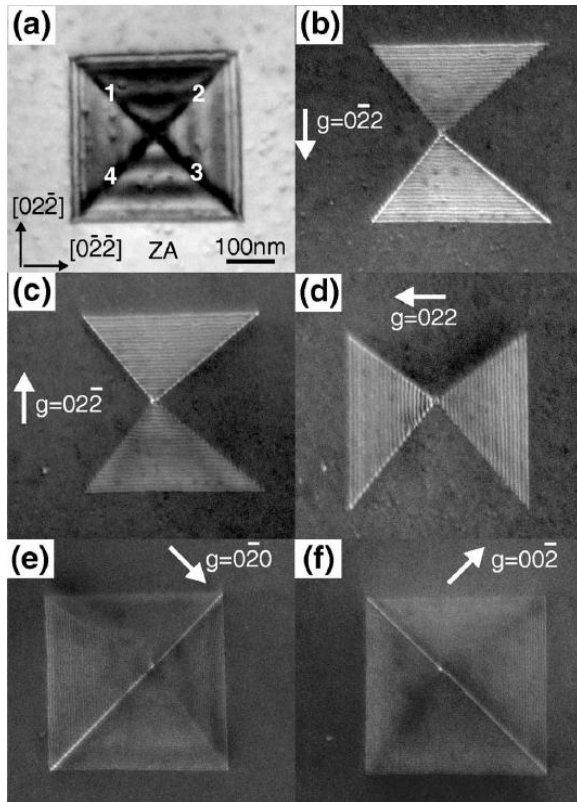


**Fig. 6.** Plan-view TEM images of a complete stacking fault pyramid. (a) [100] on-axis bright field image. (b)–(f) weak beam images under different imaging vector **g** conditions. Reprinted from *Sears et al.* [58], with the permission of © 2006 AIP Publishing.

Dislocation levels with similar properties are reported in other semiconductors [53, 62], including InGaAs/GaAs hetero-structures [63, 64], and their $E_a$ is shown to have a linear dependence on bandgap width, so their levels are concluded to be tied to the valence band. Afterwards, these dislocation levels with a logarithmic dependence of the peak amplitude *versus* $t_p$ were observed in In(Ga)As/(In)GaAs nanostructures by DLTS [28, 65–67] (Fig. 7) and PICTS [20, 68].
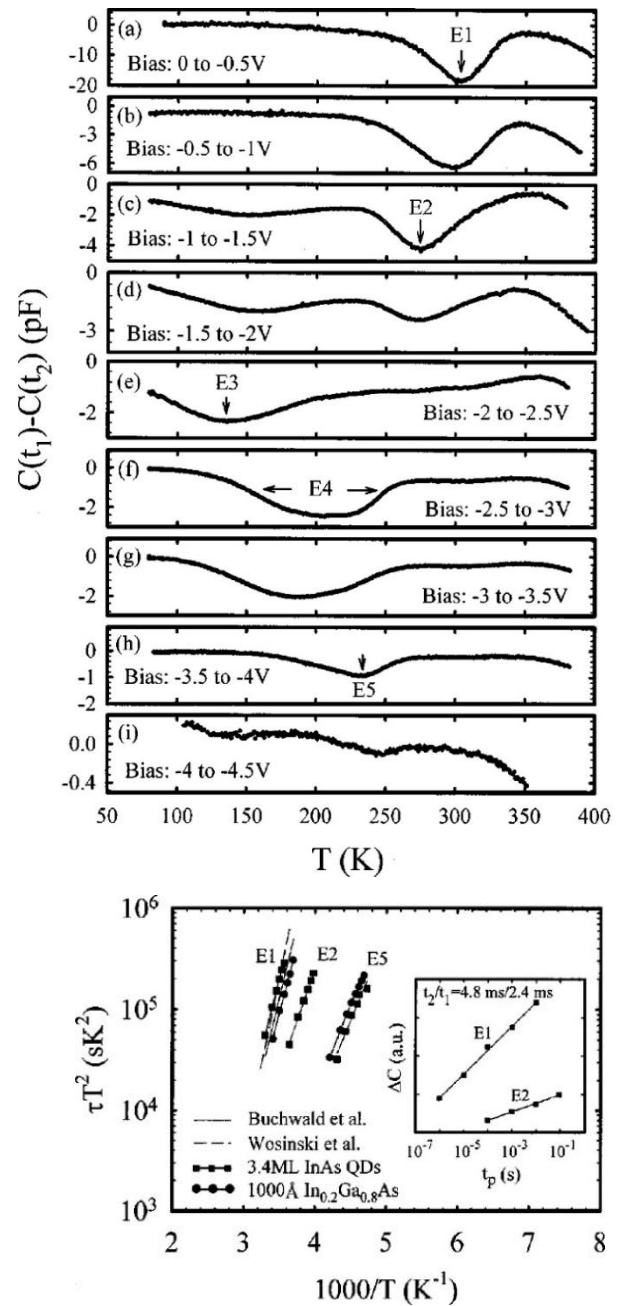


**Fig. 7.** The DLTS spectra for a InAs/GaAs QD structure. The measuring frequency is $10^5$ Hz and $t_2 / t_1$ =1.53 s/0.153 s. The Arrhenius plot of the found traps E1, E2, and E5. The inset shows the DLTS peak amplitudes of E1 and E2 traps *vs* filling-pulse duration time. Reprinted from *Wang et al.* [71], with the permission of © 2000 AIP Publishing.

The values of $E_a$ of EDs in QD heterostructures are within a rather wide range. While PICTS [20, 68] shows logarithmic functions of the peak amplitude for shallow levels with $E_a$ of 0.127 to 0.161 eV, which are comparable to the ground electron levels of In(Ga)As/GaAs QDs [69], such a dependence is also observed for deeper layers at $E_c – (0.39…0.40)$, $(0.53…0.54)$, 0.64 and 0.70 eV in DLTS spectra [64, 67, 70]. Moreover, Chen *et al.* [66] found EDs in confining layers of QD structures with $E_a$ dependent on the structure depth. They observed a decrease of electron-emission energy of a threading trap from 0.63 down to 0.36 eV, scanning from the sample surface toward the QD layer. It was explained by the trap across the QD interface, where a band offset exists.

The logarithmic dependence of amplitude on $t_p$ seems to be the most effective way to differentiate EDs from PDs that exhibit exponential (saturating) dependence [66]. Other criteria mainly involve comparison of the found defect location with the ED locations obtained from TEM cross-section images and are not so reliable, because there are many types of PDs in binary/ternary semiconductors and their energy spectrum overlap that of EDs, which are in fact the sequences of interacting PDs.

## 4. Spectrum of defect electron levels in In(Ga)As/GaAs nanostructures

We have assembled the complete information about defects in In(Ga)As/GaAs nanostructures in Table S1, Supplementary Materials. As mentioned above, a difficulty in their identification is the fact that some of them have close $E_a$ and are hardly resolved by the available methods. Moreover, the properties of a defect can be affected by environment, as a result, some traps in nanostructures reveal $E_a$ dependent on the sample depth [28, 66]. Furthermore, many known GaAs traps and recombination levels are reported as defect complexes, thus their properties can depend on the distance between the components in the crystal structure. The value of emission (capture) cross-section, being an additional parameter of defect obtainable by thermally-driven techniques, could be helpful in their identification, however, this parameter is obviously much more sensitive to the environment or the error of its estimation is very high. Anyway, the discrepancies in the values obtained for different samples are times or even orders of magnitude.

Most of the nanoobjects in the analyzed works are $In_xGa_{1–x}As$ QDs of different nominal stoichiometry with $x$ from 0 to 0.5 embedded in the GaAs matrix. However, one should consider these numbers with care, because an actual QD material is enriched by Ga [72], *e.g.*, the average value of $x$ for the nominal InAs can take values from 0.5 up to 0.8 depending on the growth conditions and, moreover, the actual stoichiometry of QD is non-uniform along the height coordinate. Also, a large number of the referred nanostructures are $In_xGa_{1–x}As$/GaAs QWs [22, 47, 67, 73–75] with a reported $x$ from 0 to 0.35,

including a superlattice [14] and $In_xGa_{1–x}As$/GaAs QWRs with a nominal $x$ of 0.3 [69, 76], 0.38 [18] and 0.4 [52].

To reduce the InAs/GaAs lattice mismatch strains and thus reduce the interface defects, neighboring InGaAs layers are embedded in the structure. For example, Chen *et al.* [21, 22, 70, 77] and Asano *et al.* [16] studied capped InAs QDs by thin $In_{0.15}Ga_{0.85}As$ layers. Kim *et al.* [78] used an InAs/InGaAs/GaAs quantum dot-in-well structure (DWEL), where an InAs QD layer was grown on a bottom 2.5 monolayer (ML) $In_{0.2}Ga_{0.8}As$ layer and covered by a top 15 ML $In_{0.2}Ga_{0.8}As$ one, while Dobbert *et al.* [79] investigated InAs QWs sandwiched between two 150 Å thick $In_{0.53}Ga_{0.47}As$ layers. Finally, Rimada *et al.* [28] and Golovynskyi *et al.* [23, 80] detected deep levels in the GaAs-based structures with InAs QDs embedded in thick (hundreds of nanometers) metamorphic InGaAs layers of different stoichiometry, sometimes QD layers were sandwiched between two thin wide-gap barrier layers [12, 81].

The deepest detected defects are EB3 and EL2. Although authors of only some works refer to EL2 while detecting the levels at $E_c – (0.71…0.9 eV)$ [9, 82, 83], all the unidentified levels within this range could be confidently attributed to this defect or EL2 family, taking into account its referred above positions in GaAs. As for the deepest unidentified level at $E_c – 1.03 eV$ observed along with 0.78 eV (EL2) by Kaniewska *et al.* [15], we tend to attribute it to EB3 [36], alike the state 0.9 eV that is observed along with EL2-related levels at 0.71 eV and 0.86 eV [9].

Localizing the defects within this range of $E_a$, most researchers detected them in In(Ga)As/GaAs structures near the QD layer [16, 56, 57, 84], part of them being found at the top of the capping GaAs layer [16, 85]. The first shallower electron trap at $E_c – 0.70 eV$ is found [84] in an $In_{0.14}Ga_{0.96}As$/GaAs QD structure and referred to a GaAs MD, namely ED1, detected first by Wosiński [60] in GaAs at a similar localization of $E_c – 0.68 eV$. Chen *et al.* found trap levels at somewhat lower energies $(0.63…0.64 eV)$ in GaAs layers capping $InAs_{0.94}Sb_{0.06}$ QDs [64] and, later, in InAs QDs [66], their belonging to EDs being established by a logarithmic dependence of the DLTS peak amplitude on $t_p$.

This trap is referred to TDs originated at the QD layer and extending towards the surface. Such kind of defects was later observed in the TEM images of InAs/GaAs structure cross-sections [56, 57, 71] together with the DLTS detection at $E_c – 0.52…0.54 eV$ in the capping layer. Furthermore, a similar trap at $E_c – 0.53 eV$ revealing a logarithmic DLTS amplitude *vs* $t_p$ is found in GaAs capping an $In_{0.2}Ga_{0.8}As$/GaAs QW and also related to TDs. It is worth noting that such a feature was observed by Prezioso *et al.* [26] for a similar trap with $E_a$ varying from 0.63 to 0.67 eV in different InAs/GaAs QD samples; the traps were mainly found near a QD layer and related to another type of EDs, namely, stacking fault tetrahedra observed in the TEM cross-sections no more than 100 nm above QDs (Fig. 6).

However, the considered range of depths is peculiar to EL3 (M5–M6 by Lang) of a GaAs lattice, so most researchers, while finding traps near In(Ga)As nanolayers from $E_c$ – 0.65 eV to $E_c$ – 0.53 eV, attributed them to PDs. Apart from EL3 (M6) [9, 27, 47] or other $V_{As}$-related defects [47, 79], PD-oxygen complexes [15, 56, 57] were assumed, since a high amount of oxygen was found by Kaniewska *et al.* [15] near the InAs QD layer, to presumably originate from oxygen-containing species produced within source cells used in molecular bean epitaxy.

The next shallower PD is EL4 (M4 by Lang) detected at $E_c$ – (0.48…0.52 eV). GaAs-based nanostructures also exhibit electron traps at similar positions detected mostly near In(Ga)As QD and QW layers. Most of them, having $E_a$ from 0.50 to 0.45 eV, are attributed just to EL4 (M4) [27, 73, 79, 86]. However, there is a reason to also suspect involvement of EDs in these levels. Gombia *et al.* [87] declared a logarithmic dependence of the DLTS peak amplitude on $t_p$ for a trap with $E_a$ of 0.48 eV found near the InAs QD layer. In addition, later papers of that research group show comparable properties for a similar trap [26] and a slightly deeper one at $E_c$ – 0.52 eV [56, 57] found in GaAs cap of InAs QDs and attributed to V-shaped TDs observed by cross-section TEM. It should be noted that the DLTS peak of the trap at 0.48 eV found in Ref. [26] was observed in the GaAs cap along with a signature of PD M4.

In the range that we relate to EL5 (0.38…0.44 eV), some researchers, finding the traps near In(Ga)As nanolayers, do refer them to PDs including EL5 [84], M4 [26, 47] and even substitution $Ni_{Ga}$ defect attributed to residual contaminants in the epitaxial growth sources [87]. Herewith, a lot of studies report the electron states in the neighboring GaAs bottom [66, 77, 87], being attributed to dislocations [66, 77], despite the fact that an exponential dependence of the DLTS response is detected in Ref. [66], which is an evidence of isolated states, unlike the logarithmic one typical for trap arrays. However, a non-exponential dependence best fitted within an assumption of 2D-distributed array is found for a trap near the InAs QD layer [88, 89], though related to PD clusters, since no dislocations are observed by cross-section TEM. However, some of the levels in this depth range are detected at the top of a GaAs layer [16, 70, 71] and also attributed to dislocations [71] like TDs [70].

In the energy interval that we attribute to EL6 ($E_c$ – (0.32…0.37 eV)), a lot of electron levels are reported near In(Ga)As nanolayers [12, 18, 23, 64, 79, 88, 89] and in a bottom GaAs [67], while Asano *et al.* [16] observed the states at the top of a GaAs cap. The trap found in the bottom buffer of an $In_{0.2}Ga_{0.8}As$/GaAs QW structure exhibits exponential dependence of the DLTS signal amplitude on $t_p$, which is an evidence for it to be isolated. Traps with a similar $E_a$ of 0.35…0.37 eV are found by the same research group [22, 77] near the InAs QD layer, capped with a 6-nm thick $In_{0.15}Ga_{0.85}As$ and neighboring GaAs bottom. Manifesting the exponential behavior of DLTS amplitude on $t_p$, the trap is

also attributed to PDs but related to MDs observed on cross-sectional TEM images [22]. In earlier works, Chen *et al.* detected electron levels at $E_c$ – (0.33…0.34 eV) near the nanolayers in InAs/GaAs QD [71] and $In_{0.2}Ga_{0.8}As$/GaAs QW [90, 91] structures and also believed them to originate from MDs. The reasons were TEM observations [71] and the fact that no DLTS signal was revealed below InGaAs critical thickness [90]. Furthermore, an evidence of the relation of EDs to a level at $E_c$ – 0.322 eV was obtained by Walther *et al.* [88, 89], who observed a dependence of the filled trap number on the DLTS filling pulse width best fitted within a 2D model of trap array. A logarithmic dependence of the DLTS signal on $t_p$, inherent in linearly-distributed arrays, is reported for the electron trap with $E_a$ ranging within 0.30…0.36 eV, depending on the InAs/GaAs QD sample parameters, which is observed near the QD layer and related to the tetrahedral stacking fault [26]. The corresponding DLTS peak is detected in addition to the one of M2 concentrated mainly in a cap, but also found in layers below.

It would be correct to associate M2 defect ($E_c$ – 0.29 eV) with EL7 ($E_c$ – 0.30 eV) or EL8 ($E_c$ – 0.275 eV). In In(Ga)As/(In)GaAs nanostructures, the levels of 0.28 to 0.32 eV are detected mostly near QD layers [18, 23, 26, 47, 79, 92] (and QW [47]) and attributed mainly to PDs. Though, Prezioso *et al.* [26], apart from M2 defect, also found a level at $E_c$ – (0.30…0.36 eV) with a logarithmic dependence of the DLTS signal amplitude on $t_p$ and related it to EDs, namely, stacking fault tetrahedra detected by TEM in a GaAs cap.

The next shallower trap EL9 ($E_c$ – (0.22…0.24 eV)) is detected in the nanostructures only by optical methods, such as photocurrent (PC) spectroscopy [9], TSC [17, 79] and PICTS [18]. No EDs are assumed as a possible origin of this trap, so it can be referred to EL9 [79], M2 [9] and $As_i$-$V_{As}$ or $As_{Ga}$-$V_{As}$ PD complexes [92] detected near QD layers [12, 18, 23, 69, 79, 80] and outside [17].

Identification of the traps with $E_a$ ranging within 0.12…0.21 eV is complicated, which is caused by insufficiently detailed classification of GaAs shallow traps. Usually they were related to M1 or EL10, however, in this spectral range, two [16, 69] or even three [20, 92] levels were often detected in one transition spectra of an In(Ga)As/GaAs sample, sometimes along with signatures of the next deeper EL9 trap ($E_c$ – (0.22…0.24 eV)) [20, 69, 92]. Possibly, a number of tabulated traps has to be extended or M1 should be considered as a family of traps. These defects are mostly detected near In(Ga)As QD [17, 47, 69, 73, 80, 81, 93] and QW layers [67, 73, 74]. As for GaAs confining layers, only Dózsa *et al.* [94] found a trap $E_c$ – 0.21 eV at a capping layer, while Asano *et al.* [16] observed the 0.16 eV trap in the GaAs bottom.

Except for PDs, EDs are reported to be responsible for three traps at $E_c$ – (0.127…0.161 eV) found in InAs/GaAs QD and QW structures by PICTS [20, 68]. The reason for this assumption is a logarithmic dependence of the PICTS response on optical excitation pulse width.

Detection of shallower electron traps with $E_a$ below 0.12 eV is relatively rare because of several reasons. Firstly, temperatures lower than nitrogen boiling one are needed to keep the traps occupied for a sufficiently long time. Secondly, shallow traps are close in depth to QD electron levels, and, being localized mainly near In(Ga)As layers (only this location is reported for the traps of this range [47, 74]), can lose electrons through tunneling into QD electron localized states with a subsequent recombination with holes. Furthermore, the DLTS signals from shallower traps could be related to those from QD levels.

In the range of Lang's defect M0 ($E_c - 0.08$ eV), only several traps are reported in In(Ga)As/GaAs nanostructures. The first one related to M0 ($E_c - 0.11$ eV) is found by Krispin *et al.* [47] near InAs QW embedded in GaAs. It should be noted that most of the researchers, who reported traps with $E_a$ below 0.12 eV, also detected the traps within 0.14…0.18 eV (the range of M1) in the same samples, therefore, confusion with deeper trap M1 could be excluded. The shallowest trap that could be related to M0 range is found in a stacked $In_{0.4}Ga_{0.6}As/$ GaAs QWR structure by Al Saqri *et al.* [53] at $E_c - (0.074 \pm 0.003$ eV). In a similar stacked sample, they also found a trap with $E_a = 0.041 \pm 0.004$ eV, which is in the range of the shallowest GaAs defect M00 and was attributed to PD $V_{As}$ being also a conventional attribution of M00. To date, this trap remains the only one found in this range of $E_a$ in GaAs-based nanostructures and is the shallowest known defect state in these structures.

## 5. Defects in metamorphic InAs/InGaAs nanostructures with QDs

Despite the promises in telecommunications, nanostructures where InAs QDs are embedded in a thick $In_xGa_{1-x}As$ metamorphic buffer are poorly studied. Seravalli *et al.* [60] studied statistics of EDs in metamorphic InAs/$In_xGa_{1-x}As$ QD structures grown on GaAs by using TEM images and found them to be different from conventional InAs/GaAs structures having V-shape dislocations in the GaAs capping layer as prevailing EDs [57, 58]. Unlike them, metamorphic structures with In content $x = 0.15$ are found to have an order less density of these defects at equivalent InAs coverage. Besides, TDs starting at the InGaAs/GaAs interface propagate across the entire InGaAs layer width, part of them reaches the surface through an 800-nm metamorphic buffer and the embedded QD layer; their density increases with $x$. Also, a new kind of EDs, named 'closed-shaped defects', is found in metamorphic structures (Fig. 5b). They are reported [60] to enclose single QDs and consist of pairs of stacking faults on (111) planes that are inclined against each other to form tetrahedral-shaped defects. These EDs are found to be predominant in metamorphic structures [28], they start to appear near QDs at InAs coverage of 2.6 ML and their amount rapidly increases with coverage as well as $x$. For example, their amount is five times higher for $x = 0.24$ than for $x = 0.15$ [60]. This kind of EDs is not detected in InAs/GaAs, though similar in shape defects, the so-called 'stacking fault tetrahedral', were found there earlier [26].

The latter are also $\Lambda$-shaped and terminate near the QD layer, however, they are more extended in all directions and can expand over 100 nm.

The electron levels of defects are studied both in vertical metamorphic InAs/$In_{0.15}Ga_{0.85}As$ QD (InAs coverage of 3.0 ML) and QW (2.0 ML) structures by DLTS [28] and lateral InAs/$In_xGa_{1-x}As$ QD structures with different $x$ by TSC [12, 23, 80, 81]. Despite the difference in the kinds of EDs, the electron states detected in these structures are those which could be found in the In(Ga)As/GaAs ones.

EL2 defects, the most studied in GaAs and rife in In(Ga)As/GaAs nanostructures, though detected in IR absorption spectra [10, 88], are not found by DLTS in vertical structures, while the substrate was out of current flow due to a special contact geometry [28]. The photoelectric spectra for this contact geometry showed no evidence of EL2. However, when the researchers involved the entire structure including the GaAs buffer MBE layer and substrate, the respective features were revealed at 0.86 and 0.72 eV in the PC [84] and photovoltage spectra [11], respectively. So, it has been concluded that the EL2 centers are related to the InGaAs/GaAs interface below rather than the metamorphic buffer and embedded QD layer. So, EL2 found as a feature at 0.74 eV in the PC spectra of GaAs-based InAs/$In_xGa_{1-x}As$ QD structures [12, 23, 80, 81] can be also a contribution of the InGaAs/GaAs interface and could not be considered as an inherent defect of these nanostructures.

As for shallower defects, their signatures are widely presented in DLTS and, especially, TCS spectra (Fig. 2) in the ranges we allocated for defects in In(Ga)As/GaAs nanostructures. It should be noted that all the DLTS bands are notably more intense for QD samples compared to QW ones.

So, two types of traps with logarithmic DLTS amplitude dependence on $t_p$ are found in metamorphic InAs/$In_{0.15}Ga_{0.85}As$ QD and QW at temperatures corresponding to $E_a$ of 0.48…0.54 eV (EL3–EL4 range). Higher energies are detected in InGaAs away from the InAs layers and attributed to TDs [28]. It should be mentioned that TDs propagating from the InGaAs/GaAs interface up to the surface are reported in addition to V-shape TDs originating from the QD layer. TSC studies [23, 80] confirmed the presence of such a trap (0.52…0.54 eV) in $In_xGa_{1-x}As$ confining layers with $x$ from 0.15 to 0.31. It is attributed to TDs or EL3-family defects related to dislocations observed mainly at the InGaAs band-to-band excitation rather than resonant QD excitation. It should be noted that the TSC technique is sensitive to the states only above the Fermi level, whereas a feature above 0.61 eV is then found in the PC spectra, indicating that defect levels could be also below $E_c - 0.54$ eV.

Returning to the ED-related traps with $E_a$ of 0.48 to 0.54 eV found by DLTS in vertical InAs/$In_{0.15}Ga_{0.85}As$ metamorphic nanostructures [28], the lower values are detected near the QD layer (InAs coverage of 3.0 ML). They could be attributed to closed-shaped defects, however, a similar band is detected for a QW sample (2.0 ML of InAs) where such kind of EDs is not observed.

MDs, usually located below In(Ga)As nanolayer embedded to GaAs, also could not be an origin of these traps near $E_c$ – 0.48 eV around InAs/InGaAs QDs and QWs, because this kind of EDs in metamorphic structure is concentrated mainly below the InGaAs/GaAs interface and not found near InAs layers [28, 60]. Thus, no ED as a reasonable origin for the trap near $E_c$ – 0.48 eV is found. Nevertheless, the trap with $E_a$ of 0.47…0.48 eV detected using TSC in lateral InAs/InGaAs QD structures, being better revealed after the resonant excitation of QDs rather than buffer band-to-band excitation, is also attributed to EDs or EL4 defects related to them.

At the same time, the trap at $E_c$ – (0.42…0.43 eV) is observed by TSC after either the InGaAs band-to-band excitation or the resonant excitation of QDs for most of the samples [23, 80]. Although, the ones with an In-rich $In_xGa_{1-x}As$ containing layer ($x$ = 0.28…0.31) exhibit signatures of this trap mainly after the excitation above the InGaAs bandgap, which is an evidence of their presence in the buffer rather than their localization near QDs. They are therefore attributed to TDs generated from the InGaAs/GaAs interface and propagating towards the sample surface or to EL5-like defects related to them. It should be noted that the DLTS studies of vertical structures [28] report no band characteristic of this defect.

Also, EL6 trap, being very rife in bulk GaAs and In(Ga)As/GaAs nanostructures, is not found in the InAs/In$_{0.15}$Ga$_{0.85}$As vertical structures by DLTS, while it is well detectable by TSC in the lateral metamorphic samples with higher In content ($x \geq 0.24$) [23, 80]. A level near $E_c$ – 0.37 eV is attributed to this trap. For most of the samples, the respective band is distinct and intense after the resonant optical excitation in QDs and is concluded to be located near the QD layer. At the same time, the response is much less distinguishable after InGaAs band-to-band pumping, being poorly detectable in the InAs/In$_{0.15}$Ga$_{0.85}$As sample after any type of excitation.

Generally, the intensity of TSC bands for any found trap is reported to decrease with $x$ in the buffer, except for the deepest one (0.52…0.54 eV) that exhibited no substantial dependence on $x$.

The next shallower trap, EL7, is found both in TSC (near 0.29…0.30 eV for different samples) and DLTS (0.29 eV) measurements. While the researchers of In(Ga)As/GaAs nanostructures found these traps mainly near In(Ga)As layers, metamorphic InAs/In$_{0.15}$Ga$_{0.85}$As structures reveal the trap $E_c$ – 0.29 eV at the top of 500-nm thick In$_{0.15}$Ga$_{0.85}$As capping layer [28]. Although TSC bands are found much stronger after the QD resonant excitation for every sample (except for $x$ = 0.15, where the buffer excitation at 1.3 eV gave a higher EL7 response), which could be an evidence of the traps to be located near QD layer, there is no contradiction with the DLTS data, taking into account a thin (20 nm) InGaAs cap in the investigated lateral metamorphic QD structures [23, 80].

Near the EL7 response, a weak shoulder is detected at lower temperatures in some TSC spectra of metamorphic structures [23, 81] and attributed to EL8 trap (0.27 eV). Another distinct peak is observed at higher temperature [23], and the trap with the respective $E_a$ = 0.31 eV is attributed to ED containing Frenkel pairs V$_{As}$-As$_i$ generated on the dislocation line. Also, similar responses of 0.30…0.31 eV are found in the TSC spectra of the metamorphic structures with InAs QDs confined by few-nanometer-thick wide-gap confining barriers [12, 81].

The trap marked in Ref. [80] as EL9 ($E_c$ – 0.23 eV) is TSC-observed much better after the resonant QD excitation for the samples with $x \geq 0.24$, though the InAs/In$_{0.15}$Ga$_{0.85}$As structure, on the contrary, reveals a better EL9 signal after the buffer excitation [12, 23, 80, 81]. Similar to In(Ga)As/GaAs structures, no EL9 response is detected in DLTS experiments [28].

At the same time, the signatures of a shallower trap are found in both kinds of transition spectroscopy measurements; $E_a$ are estimated as 0.15 eV by using DLTS [28] and 0.167 ± 0.005 eV by applying TSC [80]. This EL10-like trap is located at the top of InGaAs cap of the vertical structures [28], being observed in the TSC spectra of lateral structures mainly as a weak band at the periphery of the stronger EL9 band after the resonant excitation in QDs. M0 trap (~0.11 eV) is the shallowest trap found in the metamorphic InAs/In$_x$Ga$_{1-x}$As QD structures [23]. It is observed (Fig. 2) after long-time excitations and short-time delays in the dark before heating and localized presumably near the QD layer.

Comparing the metamorphic QD structures to the conventional In(Ga)As/GaAs nanostructures, one can conclude that both kinds of the nanostructures have similar defect levels in the bandgaps of embedding layers. Quantitative estimation of the total amount of defects in both kinds of nanostructures is carried out in Ref. [80]: a metamorphic InAs/In$_{0.15}$Ga$_{0.85}$As QD structure contains the amount of defects comparable to that in the best InGaAs/GaAs structures and, perhaps, less than in the nominal InAs/GaAs QD structures. However, the defect amount rapidly increases with In content $x$ in the buffer layer so that it is 20 times higher at $x$ = 0.31 than at $x$ = 0.15. The difference between kinds of nanostructures by defect types and amounts as well as a strong dependence of the defect amount in InAs/In$_x$Ga$_{1-x}$As structures on $x$ could be explained by a lower stacking fault energies in InGaAs than in GaAs [95].

Being based on the collected data, we suggest Table as a simplified way to preliminary identify (In)GaAs defects in the noted nanostructures by the level depths only. We should immediately note that it is just a preliminary classification for the techniques that cannot give such an important parameter as capture (emission) cross-section, which may make the identification more reliable. We also note that the suggested attribution by Martin or Lang usually means PDs, while many researchers finding the states within 0.3…0.68 eV had reasons to relate them to dislocations, and some of them [20, 68] observed evidences of EDs, when they analyzed shallower states at 0.13…0.16 eV. Thus, some of the found traps presented in Table may turn to be EDs.

## 6. Conclusions

We collected the data on EDs and PDs found in containing layers of In(Ga)As/(In)GaAs nanostructures since they had been obtained. The defects are sorted by the $E_a$ values (level positions below the bottom of the conduction band), their localization in the containing layers and attribution are also analyzed. All the found states, including those found in metamorphic InGaAs layers confining InAs QDs, are attributed to the defects inherent in GaAs. We believe that this review would be of interest for the researchers who use these or similar nanostructures.

## Supplementary Material

The supplement file contains Table S1, ordering the data on defects detected in In(Ga)As/(In)GaAs nanostructures in different reports.

## Declaration of Competing Interest

The authors declare that they have no known competing financial interests or personal relationships that could have appeared to influence the work reported in this paper.

## Acknowledgment

## References

1.  Wu J., Jiang Q., Chen S. *et al.* Monolithically integrated InAs/GaAs quantum dot mid-infrared photodetectors on silicon substrates. *ACS Photonics*. 2016. **3**, No 5. P. 749–753. https://doi.org/10.1021/acsphotonics.6b00076.

2.  Wan Y., Zhang Z., Chao R. *et al.* Monolithically integrated InAs/InGaAs quantum dot photodetectors on silicon substrates. *Opt. Express*. 2017. **25**, No 22. P. 27715. https://doi.org/10.1364/OE.25.027715.

3.  Qiao Z., Li X., Wang H. *et al.* High-performance 1.06-μm InGaAs/GaAs double-quantum-well semiconductor lasers with asymmetric heterostructure layers. *Semicond. Sci. Technol.* 2019. **34**, No 5. P. 055013. https://doi.org/10.1088/1361-6641/ab110b.

4.  Kwoen J., Imoto T., Arakawa Y. InAs/InGaAs quantum dot lasers on multi-functional metamorphic buffer layers. *Opt. Express.* 2021. **29**, No 18. P. 29378. https://doi.org/10.1364/OE.433030.

5.  Kondratenko S., Kozak O., Rozouvan S. *et al.* Carrier dynamics and recombination in silicon doped InAs/GaAs quantum dot solar cells with AlAs cap layers. *Semicond. Sci. Technol.* 2020. **35**, No 11. P. 115018. https://doi.org/10.1088/1361-6641/abb1c7.

6.  Seravalli L. Metamorphic InAs/InGaAs quantum dots for optoelectronic devices: A review. *Microelectron. Eng*. 2023. **276**. P. 111996. https://doi.org/10.1016/j.mee.2023.111996.

7.  Rouis W., Haggui M., Rekaya S. *et al.* Local photo-current mapping of InAs/InGaAs/GaPts inter-mediate-band solar cells using scanning near-field optical microscopy. *Sol. Energy Mater. Sol. Cells*. 2016. **144**. P. 324–330. https://doi.org/10.1016/j.solmat.2015.09.026.

8.  Dai Y., Polly S.J., Hellstroem S. *et al.* Effect of electric field on carrier escape mechanisms in quantum dot intermediate band solar cells. *J. Appl. Phys.* 2017. **121**. P. 013101. https://doi.org/10.1063/1.4972958.

9.  Golovynskyi S.L., Mazur Y.I., Wang Z.M. *et al.* Excitation intensity dependence of lateral photocurrent in InGaAs/GaAs dot-chain structures. *Phys. Lett. A*. 2014. **378**, No 35. P. 2622–2626. http://doi.org/10.1016/j.physleta.2014.07.010.

10. Golovynskyi S.L., Seravalli L., Trevisi G. *et al.* Photoelectric properties of the metamorphic InAs/InGaAs quantum dot structure at room temperature. *J. Appl. Phys.* 2015. **117**, No 21. P. 214312. http://doi.org/10.1063/1.4922246.

11. Golovynskyi S., Seravalli L., Datsenko O. *et al.* Bipolar effects in photovoltage of metamorphic InAs/InGaAs/GaAs quantum dot heterostructures: Characterization and design solutions for light-sensitive devices. *Nanoscale Res. Lett*. 2017. **12**. P. 559. http://doi.org/10.1186/s11671-017-2331-2.

12. Golovynskyi S., Datsenko O.I., Seravalli L. *et al.* InAs/InGaAs quantum dots confined by InAlAs barriers for enhanced room temperature light emission: Photoelectric properties and deep levels. *Microelectron. Eng.* 2021. **238**. P. 111514. https://doi.org/10.1016/j.mee.2021.111514.

13. Datsenko O.I., Golovynskyi S., Suárez I. *et al.* Metamorphic InAs/InAlAs/InGaAs quantum dots: Establishing the limit for indium composition in InGaAs buffers. *Microelectron. Eng.* 2022. **263**. P. 111840. https://doi.org/10.1016/j.mee.2022.111840.

14. Dhar S., Das U., Bhattacharya P.K. Deep levels in as-grown and Si-implanted $In_{0.2}Ga_{0.8}As$–GaAs strained-layer superlattice optical guiding structures. *J. Appl. Phys.* 1986. **60**, No 2. P. 639–642. https://doi.org/10.1063/1.337406.

15. Kaniewska M., Engström O., Barcz A., Pacholak-Cybulska M. Deep levels induced by InAs/GaAs quantum dots. *Mater. Sci. Eng. C*. 2006. **26**, No 5–7. P. 871–875. https://doi.org/10.1016/j.msec.2005.09.030.

16. Asano T., Fang Z., Madhukar A. Deep levels in GaAs(001)/InAs/InGaAs/GaAs self-assembled quantum dot structures and their effect on quantum dot devices. *J. Appl. Phys.* 2010. **107**, No 7. P. 073111. http://doi.org/10.1063/1.3359704.

17. Vakulenko O.V., Golovynskyi S.L., Kondratenko S.V. Effect of carrier capture by deep levels on lateral photoconductivity of InGaAs/GaAs quantum dot structures. *J. Appl. Phys.* 2011. **110**, No 4. P. 043717. http://doi.org/10.1063/1.3626051.

18. Iliash S.A., Kondratenko S.V., Yakovliev A. *et al.* Thermally stimulated conductivity in InGaAs/GaAs quantum wire heterostructures. *SPQEO*. 2016. **19**, No 1. P. 75–78.
https://doi.org/10.15407/spqeo19.01.075.

19. Golovynskyi S.L., Dacenko O.I., Kondratenko S.V. *et al.* Intensity-dependent nonlinearity of the lateral photoconductivity in InGaAs/GaAs dot-chain structures. *J. Appl. Phys.* 2016. **119**, No 18. P. 184303. http://doi.org/10.1063/1.4948953.

20. Park C.J., Kim H.B., Lee Y.H. *et al.* Deep level defects of InAs quantum dots grown on GaAs by molecular beam epitaxy. *J. Cryst. Growth*. 2001. **227**–**228**. P. 1057–1061.
http://doi.org/10.1016/S0022-0248(01)00988-5.

21. Chen J.F., Yang C.H., Wu Y.H. *et al.* Strain relaxation in InAs self-assembled quantum dots induced by a high N incorporation. *J. Appl. Phys.* 2008. **104**, No 10. P. 103717. http://doi.org/10.1063/1.3028235.

22. Kunets V.P., Morgan T.A., Mazur Y.I. *et al.* Deep traps in GaAs/InGaAs quantum wells and quantum dots, studied by noise spectroscopy. *J. Appl. Phys.* 2008. **104**, No 10. P. 103709.
http://doi.org/10.1063/1.3020532.

23. Golovynskyi S., Datsenko O.I., Seravalli L. *et al.* Defect influence on in-plane photocurrent of InAs/InGaAs quantum dot array: long-term electron trapping and Coulomb screening. *Nanotechnology*. 2019. **30**, No 30. P. 305701.
https://doi.org/10.1088/1361-6528/ab1866.

24. Uchida Y., Kakibayashi H., Goto S. Electrical and structural properties of dislocations confined in a InGaAs/GaAs heterostructure. *J. Appl. Phys.* 1993. **74**, No 11. P. 6720–6725.
http://doi.org/10.1063/1.355068.

25. Kim J.S., Kim E.K., Kim J.O. *et al.* Study on carrier trapping and emission processes in InAs/GaAs self-assembled quantum dots by varying filling pulse width during DLTS measurements. *Superlattices Microstruct.* 2009. **46**, No 1–2. P. 312–317. http://doi.org/10.1016/j.spmi.2009.01.011.

26. Prezioso M., Gombia E., Mosca R. *et al.* Study of electrically active defects in GaAs/InAs/GaAs QDs structures by DLTS and TEM. *Int. Conf. on Advanced Semiconductor Devices and Microsystems*. 2006. P. 237–240.
http://doi.org/10.1109/ASDAM.2006.331197.

27. Fang Z.Q., Xie Q.H., Look D.C. *et al.* Electrical characterization of self-assembled $In_{0.5}Ga_{0.5}As$/ GaAs quantum dots by deep level transient spectroscopy. *J. Electron. Mater.* 1999. **28**, No 8. P. L13–L16. https://doi.org/10.1007/s11664-999-0210-z.

28. Rimada J.C., Prezioso M., Nasi L. *et al.* Electrical and structural characterization of InAs/InGaAs quantum dot structures on GaAs. *Mater. Sci. Eng. B*. 2009. **165**, No 1–2. P. 111–114.
https://doi.org/10.1016/j.mseb.2008.10.007.

29. Lang D.V. Deep-level transient spectroscopy: A new method to characterize traps in semiconduc-tors. *J. Appl. Phys*. 1974. **45**, No 7. P. 3023–3032. https://doi.org/10.1063/1.1663719.

30. Lang D.V., Cho A.Y., Gossard A. C. *et al.* Study of electron traps in *n*-GaAs grown by molecular beam epitaxy. *J. Appl. Phys.* 1976. **47**, No 6. P. 2558–2564. http://doi.org/10.1063/1.322974.

31. Martin G.M., Mitonneau A., Mircea A. Electron traps in bulk and epitaxial GaAs crystals. *Electron. Lett.* 1977. **13**, No 7. P. 191.
https://doi.org/10.1049/el:19770140.

32. Kaminska M. Optical properties of EL2. *Rev. Phys. Appl.* 1988. **23**, No 5. P. 793–802. https://doi.org/ 10.1051/rphysap:019880023050793000.

33. von Bardeleben H.J., Stiévenard D., Deresmes D. *et al.* Identification of a defect in a semiconductor: EL2 in GaAs. *Phys. Rev. B*. 1986. **34**, No 10. P. 7192–7202.
https://doi.org/10.1103/PhysRevB.34.7192.

34. Reddy C.V., Fung S., Beling C.D. Nature of the bulk defects in GaAs through high-temperature quenching studies. *Phys. Rev. B*. 1996. **54**, No 16. P. 11290–11297. https://doi.org/10.1103/PhysRevB.54.11290.

35. Oyama Y., Nishizawa J.-I. Excitation photo-capacitance study of EL2 in *n*-GaAs prepared by annealing under different arsenic vapor pressures. *J. Appl. Phys.* 2005. **97**, No 3. P. 031101. https://doi.org/10.1063/1.1843271.

36. Bacuyag D., Escaño M.C.S., David M., Tani M. First-principles study of structural, electronic, and optical properties of surface defects in GaAs(001) – β2(2×4). *AIP Adv.* 2018. **8**, No 6. P. 065012. https://doi.org/10.1063/1.5020188.

37. Neild S.T., Skowronski M., Lagowski J. Signature of the gallium-oxygen-gallium defect in GaAs by deep level transient spectroscopy measurements. *Appl. Phys. Lett.* 1991. **58**, No 8. P. 859–861. http://doi.org/10.1063/1.104513.

38. Xia J., Mandelis A. Radiative defect state identification in semi-insulating GaAs using photocarrier radiometry. *Semicond. Sci. Technol.* 2009. **24**, No 12. P. 125002. http://doi.org/10.1088/0268-1242/24/12/125002.

39. Fang Z., Shan L., Schlesinger T.E., Milnes A.G. Study of defects in LEC-grown undoped SI-GaAs by thermally stimulated current spectroscopy. *Mater. Sci. Eng. B*. 1990. **5**, No 3. P. 397–408. http://doi.org/10.1016/0921-5107(90)90104-J.

40. Gelczuk Ł., Kopaczek J., Rockett T.B.O. *et al.* Deep-level defects in *n*-type GaAsBi alloys grown by molecular beam epitaxy at low temperature and their influence on optical properties. *Sci. Rep.* 2017. **7**, No 1. P. 12824. http://doi.org/10.1038/s41598-017-13191-9.

41. Fang Z.Q., Schlesinger T.E., Milnes A.G. Evidence for EL6 ($E_c$ − 0.35 eV) acting as a dominant recombination center in *n*-type horizontal Bridgman GaAs. *J. Appl. Phys.* 1987. **61**, No 11. P. 5047–5050. http://doi.org/10.1063/1.338327.

42. Yakimova R., Paskova T., Hardalov C. Behavior of an EL5-like defect in metalorganic vapor-phase epitaxial GaAs:Sb. *J. Appl. Phys.* 1993. **74**, No 10. P. 6170–6173. https://doi.org/10.1063/1.355184.

43. Shiraki H., Tokuda Y., Sassa K. Bistable behavior of a medium-deep center related to EL5 and EL6 in *n*-type bulk GaAs. *J. Appl. Phys.* 1998. **84**, No 6. P. 3167–3174. http://doi.org/10.1063/1.368514.

44. Lai S.T., Nener B.D., Faraone L. *et al.* Characterization of deep-level defects in GaAs irradiated by 1 MeV electrons. *J. Appl. Phys.* 1993. **73**, No 2. P. 640–647. http://doi.org/10.1063/1.353375.

45. Blood P., Harris J.J. Deep states in GaAs grown by molecular beam epitaxy. *J. Appl. Phys.* 1984. **56**, No 4. P. 993–1007. http://doi.org/10.1063/1.334040.

46. Reddy C.V., Luo Y.L., Fung S., Beling C.D. DX-like properties of the EL6 defect family in GaAs. *Phys. Rev. B*. 1998. **58**, No 3. P. 1358–1366. https://doi.org/10.1103/PhysRevB.58.1358.

47. Krispin P., Lazzari J.L., Kostial H. Deep and shallow electronic states at ultrathin InAs insertions in GaAs investigated by capacitance spectroscopy. *J. Appl. Phys.* 1998. **84**, No 11. P. 6135–6140. http://doi.org/10.1063/1.368927.

48. Fang Z.Q., Yamamoto H., Look D.C. Origin and behavior of main electron traps in Si-implanted GaAs. *MRS Proc.* 2011. **184**. P. 93–98. https://doi.org/10.1557/PROC-184-93.

49. Deenapanray P.N.K., Tan H.H., Jagadish C., Auret F.D. Investigation of deep levels in rapid thermally annealed $SiO_2$-capped *n*-GaAs grown by metal-organic chemical vapor deposition. *Appl. Phys. Lett.* 2000. **77**. No 5. P. 696–698. https://doi.org/10.1063/1.127089.

50. Bourgoin J.C., von Bardeleben H.J., Stiévenard D. Native defects in gallium arsenide. *J. Appl. Phys.* 1988. **64**, No 9. P. R65–R92. https://doi.org/10.1063/1.341206.

51. Corbel C., Stucky M., Hautojärvi P. *et al.* Positron-annihilation spectroscopy of native vacancies in as-grown GaAs. *Phys. Rev. B.* 1988. **38**, No 12. P. 8192–8208. https://doi.org/10.1103/PhysRevB.38.8192.

52. DeJule R.Y., Haase M.A., Stillman G.E. *et al.* Measurements of deep levels in high-purity molecular beam epitaxial GaAs. *J. Appl. Phys.* 1985. **57**, No 12. P. 5287–5289. https://doi.org/10.1063/1.334843.

53. Al Saqri N.A., Felix J.F., Aziz M. *et al.* Investigation of electrically active defects in InGaAs quantum wire intermediate-band solar cells using deep-level transient spectroscopy technique. *Nanotechnology.* 2017. **28**, No 4. P. 045707. http://doi.org/10.1088/1361-6528/28/4/045707

54. Yastrubchak O., Wosiński T., Mąkosa A. *et al.* Capture kinetics at deep-level defects in lattice-mismatched GaAs-based heterostructures. *Physica B: Condens. Matter.* 2001. **308**–**310**. P. 757–760. https://doi.org/10.1016/S0921-4526(01)00828-6.

55. Jin-Phillipp N.Y., Phillipp F. Defect formation in self-assembling quantum dots of InGaAs on GaAs: a case study of direct measurements of local strain from HREM. *J. Microsc.* 2001. **194**, No 1. P. 161–170. https://doi.org/10.1046/j.1365-2818.1999.00472.x.

56. Lytvyn P.M., Mazur Y.I., Marega E., Jr *et al.* Engineering of 3D self-directed quantum dot ordering in multilayer InGaAs/GaAs nanostructures by means of flux gas composition. *Nanotechnology.* 2008. **19**, No 50. P. 505605. https://doi.org/10.1088/0957-4484/19/50/505605.

57. Frigeri P., Nasi L., Prezioso M. *et al.* Effects of the quantum dot ripening in high-coverage InAs⁄GaAs nanostructures. *J. Appl. Phys.* 2007. **102**, No 8. P. 083506. http://doi.org/10.1063/1.2795661.

58. Nasi L., Bocchi C., Germini F. *et al.* Defects in nano-structures with ripened InAs/GaAs quantum dots. *J. Mater. Sci.: Mater. Electron.* 2008. **19**. P. S96–S100. https://doi.org/10.1007/s10854-008-9657-6.

59. Sears K., Wong-Leung J., Tan H.H., Jagadish C. A transmission electron microscopy study of defects formed through the capping layer of self-assembled InAs⁄GaAs quantum dot samples. *J. Appl. Phys.* 2006. **99**, No 11. P. 113503. https://doi.org/10.1063/1.2197038.

60. Seravalli L., Frigeri P., Nasi L. *et al.* Metamorphic quantum dots: Quite different nanostructures. *J. Appl. Phys.* 2010. **108**, No 6. P. 064324. https://doi.org/10.1063/1.3483249.

61. Wosiński T. Evidence for the electron traps at dislocations in GaAs crystals. *J. Appl. Phys.* 1989. **65**, No 4. P. 1566–1570. http://doi.org/10.1063/1.342974.

62. Wosiński T., Mąkosa A., Figielski T., Raczyńska J. Deep levels caused by misfit dislocations in GaAsSb/GaAs heterostructures. *Appl. Phys. Lett.* 1995. **67**, No 8. P. 1131–1133. https://doi.org/10.1063/1.114984.

63. Watson G.P., Ast D.G., Anderson T.J. *et al.* The measurement of deep level states caused by misfit dislocations in InGaAs/GaAs grown on patterned GaAs substrates. *J. Appl. Phys.* 1992. **71**, No. 7. P. 3399–3407. http://doi.org/10.1063/1.350936.

64. Pal D., Gombia E., Mosca R. *et al.* Deep levels in virtually unstrained InGaAs layers deposited on GaAs. *J. Appl. Phys.* 1998. **84**, No 5. P. 2965–2967. http://doi.org/10.1063/1.368404.

65. Chen J.F., Hsiao R.S., Huang W.D. *et al.* Strain relaxation and induced defects in InAsSb self-assembled quantum dots. *Appl. Phys. Lett.* 2006. **88**, No 23. P. 233113. http://doi.org/10.1063/1.2212064.

66. Chen J.F., Wang J.S. Electron emission properties of relaxation-induced traps in InAs/GaAs quantum dots and the effect of electronic band structure. *J. Appl. Phys.* 2007. **102**, No 4. P. 043705. http://doi.org/10.1063/1.2770817.

67. Chen J.F., Chiang C.H., Hsieh P.C., Wang J.S. Analysis of strain relaxation in GaAs/InGaAs/GaAs

structures by spectroscopy of relaxation-induced states. *J. Appl. Phys.* 2007. **101**, No 3. P. 033702. http://doi.org/10.1063/1.2433771.

68. Cho H.Y. Defect states in InAs quantum dots characterized by photo-induced current transient spectroscopy. *Defect and Diffusion Forum.* 2002. **210-212**. P. 81–88. https://doi.org/10.4028/www.scientific.net/DDF.210-212.81.

69. Kondratenko S.V., Vakulenko O.V., Mazur Y.I. *et al.* Deep level centers and their role in photo-conductivity transients of InGaAs/GaAs quantum dot chains. *J. Appl. Phys.* 2014. **116**, No 19. P. 193707. http://doi.org/10.1063/1.4902311.

70. Chen J.-F., Hsiao R.-S., Shih S.-H. *et al.* Properties of defect traps in triple-stack InAs/GaAs quantum dots and effect of annealing. *Jpn. J. Appl. Phys.* 2004. **43**, No 9A/B. P. L1150–L1153. http://doi.org/10.1143/JJAP.43.L1150.

71. Wang J.S., Chen J.F., Huang J.L. *et al.* Carrier distribution and relaxation-induced defects of InAs/GaAs quantum dots. *Appl. Phys. Lett.* 2000. **77**, No 19. P. 3027–3029. http://doi.org/10.1063/1.1323735.

72. Mazur Y.I., Wang Z.M., Salamo G.J. *et al.* Investigation of indium distribution in InGaAs/GaAs quantum dot stacks using high-resolution X-ray diffraction and Raman scattering. *J. Appl. Phys.* 2006. **99**, No 2. P. 023517. https://doi.org/10.1063/1.2163009.

73. Lin S.W., Balocco C., Missous M. *et al.* Coexistence of deep levels with optically active InAs quantum dots. *Phys. Rev. B.* 2005. **72**, No 16. P. 165302. https://doi.org/10.1103/PhysRevB.72.165302.

74. Kaniewska M., Engström O., Kaczmarczyk M. Classification of energy levels in quantum dot structures by depleted layer spectroscopy. *J. Electron. Mater.* 2010. **39**, No 6. P. 766–772. https://doi.org/10.1007/s11664-010-1125-4.

75. Gelczuk Ł., Dąbrowska-Szata M., Pucicki D. DLTS investigations of (Ga,In)(N,As)/GaAs quantum wells before and after rapid thermal annealing. *Acta Physica Polonica A.* 2014. **126**, No 5. P. 1195–1198. https://doi.org/10.12693/APhysPolA.126.1195.

76. Kondratenko S.V., Iliash S.A., Vakulenko O.V. *et al.* Photoconductivity relaxation mechanisms of InGaAs/GaAs quantum dot chain structures. *Nanoscale Res. Lett.* 2017. **12**. P. 183. https://doi.org/10.1186/s11671-017-1954-7.

77. Chen J.F., Hsiao R.S., Chen Y.P. *et al.* Strain relaxation in InAs/InGaAs quantum dots investigated by photoluminescence and capacitance-voltage profiling. *Appl. Phys. Lett.* 2005. **87**, No 14. P. 141911. https://doi.org/10.1063/1.2081132.

78. Kim J.S., Kim E.K., Choi W.J. *et al.* Electrical properties of InAs/InGaAs/GaAs quantum-dot infrared photodetectors. *Jpn. J. Appl. Phys.* 2006. **45**, No 6B. P. 5575–5577. https://doi.org/10.1143/JJAP.45.5575.

79. Dobbert J., Kunets V.P., Morgan T.A. *et al.* Investigation of deep levels in InGaAs channels comprising thin layers of InAs. *J. Mater. Sci. Mater. Electron.* 2007. **19**, No 8–9. P. 797–800. http://doi.org/10.1007/s10854-007-9451-x.

80. Golovynskyi S., Datsenko O.I., Seravalli L. *et al.* Deep levels in metamorphic InAs/InGaAs quantum dot structures with different composition of the embedding layers. *Semicond. Sci. Technol.* 2017. **32**, No 12. P. 125001. https://doi.org/10.1088/1361-6641/aa91e7.

81. Golovynskyi S., Datsenko O.I., Seravalli L. *et al.* Photoelectric and deep level study of metamorphic InAs/InGaAs quantum dots with GaAs confining barriers for photoluminescence enhancement. *Semicond. Sci. Technol.* 2020. **35**, No 9. P. 095022. https://doi.org/10.1088/1361-6641/ab9db4.

82. Strong W.H., Forbes D.V., Hubbard S.M. Investigation of deep level defects in electron irradiated indium arsenide quantum dots embedded in a gallium arsenide matrix. *Mater. Sci. Semicond. Proc.* 2014. **25**. P. 76–83. https://doi.org/10.1016/j.mssp.2014.01.034.

83. Sato S.-I., Schmieder K.J., Hubbard S.M. *et al.* Defects in GaAs solar cells with InAs quantum dots created by proton irradiation. *2015 IEEE 42nd Photovoltaic Specialist Conference* (*PVSC*), 2015. P. 1–5. https://doi.org/10.1109/pvsc.2015.7355868.

84. Golovynskyi S., Seravalli L., Datsenko O. *et al.* Comparative study of photoelectric properties of metamorphic InAs/InGaAs and InAs/GaAs quantum dot structures. *Nanoscale Res. Lett.* 2017. **12**. P. 335. http://doi.org/10.1186/s11671-017-2091-z.

85. Panepinto L., Zeimer U., Seifert W. *et al.* Temperature dependent EBIC and deep level transient spectroscopy investigation of different types of misfit-dislocations at MOVPE grown GaAs/InGaAs/GaAs-single-quantum wells. *Mater. Sci. Eng. B.* 1996. **42**, No 1–3. P. 77–81. https://doi.org/10.1016/S0921-5107(96)01686-8.

86. Lee K.S., Lee D.U., Kim E.K., Choi W.J. Effect of space layer doping on photoelectric conversion efficiency of InAs/GaAs quantum dot solar cells. *Appl. Phys. Lett.* 2015. **107**, No 20. P. 203503. http://doi.org/10.1063/1.4935940.

87. Gombia E., Mosca R., Frigeri P. *et al.* Electrical characterization of self-assembled InAs/GaAs quantum dots by capacitance techniques. *Mater. Sci. Eng. B.* 2002. **91**–**92**. P. 393–397. https://doi.org/10.1016/S0921-5107(01)01028-5.

88. Walther C., Bollmann J., Kissel H. *et al.* Non-exponential capture of electrons in GaAs with embedded InAs quantum dots. *Physica B: Condensed Matter.* 1999. **273**–**274**, P. 971–975. https://doi.org/10.1016/S0921-4526(99)00604-3.

89. Walther C., Bollmann J., Kissel H. *et al.* Characterization of electron trap states due to InAs quantum dots in GaAs. *Appl. Phys. Lett.* 2000. **76**, No 20. P. 2916–2918. http://doi.org/10.1063/1.126516.

90. Chen J.F., Wang P.Y., Tsai C.Y. *et al.* Observation of carrier depletion and emission effects on capacitance dispersion in relaxed In$_{0.2}$Ga$_{0.8}$As/GaAs quantum wells. *Appl. Phys. Lett.* 1999. **75**, No 16. P. 2461–2463. https://doi.org/10.1063/1.125048.

91. Chen J.F., Wang P.Y., Wang J.S. *et al.* Carrier depletion by defects levels in relaxed In$_{0.2}$Ga$_{0.8}$As/GaAs quantum-well Schottky diodes. *J. Appl. Phys.* 2000. **87**, No 3. P. 1369–1373. http://doi.org/10.1063/1.372022.

92. Vakulenko O.V., Golovynskyi S.L., Kondratenko S.V. *et al.* Effect of interface defect states on photoelectric properties of In$_x$Ga$_{1-x}$As/GaAs heterostructures with quantum dots. *Ukr. J. Phys.* 2011. **56**, No 9. P. 940. https://doi.org/10.15407/ujpe56.9.940.

93. Sobolev M.M., Nevedomskii V.N., Zolotareva R.V. *et al.* Deep-level transient spectroscopy of InAs/GaAs quantum dot superlattices. *AIP Conf. Proc.* 2014. **1583**. P. 248–251. http://doi.org/10.1063/1.4865646.

94. Dózsa L., Horváth Z.J., Vo V.T. *et al.* The effect of InAs quantum layer and quantum dots on the electrical characteristics of GaAs structures. *Microelectron. Eng.* 2000. **51–52**. P. 85–92. https://doi.org/10.1016/S0167-9317(99)00469-4.

95. Takeuchi S., Suzuki K. Stacking fault energies of tetrahedrally coordinated crystals. *phys. status solidi (a).* 1999. **171**, No 1. P. 99–103. https://doi.org/10.1002/(SICI)1521-396X(199901)171:1<99::AID-PSSA99>3.0.CO;2-B.

## Authors' contributions

**Datsenko O.I.:** conceptualization, data curation, writing – original draft, visualization, writing – review & editing.

**Kravchenko V.M.:** validation, visualization, writing – review & editing.

**Golovynskyi S.:** conceptualization, writing – original draft, validation, supervision, writing – review & editing.

## Authors and CV

**Oleksandr Datsenko** born in 1971, he defended his Ph.D. thesis in Physics and Mathematics (Optics and Laser Physics) in 1999 at the Taras Shevchenko National University of Kyiv. He is a senior researcher at Physics Dept. of the same university. Author of over 190 scientific publications, 3 textbooks. The area of his scientific interests includes optics of semiconductors, nanomaterials and nanostructures. https://orcid.org/0000-0002-4461-1925. E-mail: oleksandr.datsenko@knu.ua.

**Vladyslav Kravchenko** born in 1971, he defended his Ph.D. thesis in Physics and Mathematics (Optics and Laser Physics) in 2000 at the Taras Shevchenko National University of Kyiv. He is an associate professor at Physics Dept. of the same university. Author of over 100 scientific publications, 6 textbooks. The area of his scientific interests includes optics of semiconductors and biophotonics. https://orcid.org/0009-0001-1315-416X. E-mail: kravm@knu.ua.

**Sergii Golovynskyi** born in 1985, he defended his Ph.D. thesis in Physics and Mathematics (Optics, Laser Physics) in 2012 at the Taras Shevchenko National University of Kyiv. In 2012, he started his research carrier at the V. Lashkaryov Institute of Semiconductor Physics, NAS of Ukraine. Since 2016, he is an associate researcher at Shenzhen University, China. Author of more than 60 scientific articles, obtaining an H-index of 18. His main research activity is in the fields of semiconductor physics and optics, spectroscopy, nanomaterials and optoelectronics. https://orcid.org/0000-0002-1864-976X.

## Електронні рівні дефектів у наноструктурах In(Ga)As/(In)GaAs: огляд

### О.І. Даценко, В.М. Кравченко, С. Головинський

**Анотація.** Систематизовано дані про електронні рівні, індуковані дефектами в наноструктурах In(Ga)As/(In)GaAs, їхню локалізацію, енергію активації та ідентифікацію. Перераховано точкові дефекти, властиві GaAs і виявлені в наноструктурах на основі (In)GaAs, а також уточнено їх класифікацію, включаючи EB3, EL2, EL3, EL4 (M4), EL5, EL6 (M3), EL7, EL8, EL9 (M2), EL10 (M1), EL11 (M0) і M00. Описано вплив інтерфейсів на формування різних типів протяжних дефектів. Усі рівні електронних пасток, виявлені в гетероструктурах із квантовими ямами, нанодротинками та точками за допомогою спектроскопії глибоких рівнів, зібрані в таблицю із зазначенням методики виявлення, об'єкта, розташування в структурі та припущенням про їхнє походження. Цей огляд може бути корисним як довідковий матеріал для дослідників, які вивчають такі наноструктури.

**Ключові слова:** InAs/GaAs, наногетероструктури, дефект, електронний стан, спектроскопія глибоких рівнів.